

Adsorptive Removal of Reactive Orange 122 from Aqueous Solutions by Ionic Liquid Coated Fe₃O₄ Magnetic Nanoparticles as an Efficient Adsorbent

Ahmadi, Seyyed Hamid*⁺; Davar, Parastoo; Manbohi, Ahmad

Chemistry & Chemical Engineering Research Center of Iran, P.O. Box 14334-186 Tehran, I.R. IRAN

ABSTRACT: In the present investigation, a novel adsorbent, ionic liquid modified magnetic nanoparticles (IL-Fe₃O₄), was successfully synthesized and characterized by FT-IR spectroscopy, ThermoGravimetric Analysis (TGA), XRD analysis, Scanning Electron Microscopy (SEM) and theory of Brunauer, Emmett, and Teller (BET) for removal of Reactive Orange 122 (RO-122) from aqueous solutions. The effects of various experimental parameters such as pH, contact time, nanoparticle dosage and ionic liquid amount were studied and optimized. Experimental results indicated that the IL-Fe₃O₄ nanoparticles had removed more than 98% of proposed dye under the optimum conditions. Detection and quantification limits of the proposed method were 14 and 46 µg/L, respectively. Desorption process of the adsorbed dye was also investigated using methanol, ethanol and propanol as the solvent. Both the adsorption and desorption of dye were quite fast. The adsorption process preferably followed the Freundlich isotherm and pseudo-second-order kinetic model. The RO-122 was removed successfully from environmental water samples too.

KEY WORDS: Reactive orange 122, magnetic nanoparticles, ionic liquid, adsorption.

INTRODUCTION

At present more than 9000 types of dyes have been incorporated in the color index and these compounds are used in large quantity in various areas such as textile, leather, paper, cosmetics, plastics, pharmaceuticals, food, etc [1]. Discharge of dyes into water sources threatens the water supply and quality due to non-degradability under harsh conditions, toxicity, accumulation and magnification throughout the food chain. The highly colored effluent not only causes damage to aquatic life but also human beings by producing carcinogenic and mutagenic effects [2]. Dyes usually have complex aromatic structures which make them stable and difficult to decompose.

The dyes present in wastewater absorb sunlight, leading to a decrease in the efficiency of photosynthesis in aquatic plants due to reduced light penetration [3]. Color removal from wastes has been the target of great attention in the environmental field because of large scale production and extensive application of synthetic dyes. Over years, a wide range of physical and chemical processes such as flocculation, electro-flotation, precipitation, electro-kinetic coagulation, ion exchange, membrane filtration, oxidation, irradiation and ozonation have been investigated extensively for removing dyes from aquatic bodies but these methods possess drawbacks

* To whom correspondence should be addressed.

+ E-mail: ahmadi@ccerci.ac.ir

1021-9986/16/1/63

11/\$/3.10

due to their inapplicability to large scale units along with both energy and chemical intensiveness [4]. Reviewing the available literature indicated that the adsorption is one of the most investigated techniques for dye removal in terms of cost, simplicity of design, ease of operation and high level of effectiveness as well as the availability of a wide range of adsorbents [5-8]. Thus, many researchers throughout the world have focused their efforts on optimizing the adsorption process and developing novel alternative adsorbents with high adsorptive capacity and low cost. In this regard, comprehensive investigations and developments were paid to Magnetic NanoParticles (MNPs), due to the high specific surface area and the absence of internal diffusion resistance [9]. Numerous chemical methods can be used to synthesize Fe_3O_4 nanoparticles. Co-precipitation, thermal decomposition, and hydrothermal synthesis, have been applied and reviewed for the production of Fe_3O_4 nanoparticles [10, 11]. Among these methods, co-precipitation is a facile and convenient pathway to obtain magnetic particles [12]. Surface modification of MNPs is a challenged key for different applications and can be accomplished by physical/chemical adsorption of organic compounds by four major methods: organic vapor condensation, polymer coating, surfactant adsorption and direct silanation [13]. In the preparation and storage of NPs in colloidal form, the stability of the colloid is of utmost importance. The NPs which have hydrophobic surfaces with a large surface area to volume ratio, tend to agglomerate in order to reduce their surface energy and form large clusters, resulting in increased particle size [14, 15]. These clusters, then, exhibit strong magnetic dipole-dipole attractions and show ferromagnetic behavior. Modification of the NPs surface is a solution to prevent this phenomenon. Selective removal of toxic target compounds from complex environmental matrices can be obtained when certain special functional ligands with affinities for target molecules are bound onto these MNPs. Therefore, present study introduces an ionic liquid (IL) as surface modifier. Nowadays, ionic liquids are widely recognized solvents due to their extended list of excellent properties and have attracted extensive attention and gained popularity in analytical chemistry [16-19].

In the proposed procedure, IL- Fe_3O_4 were produced by the adsorption of 1-tetradecyl 3-methyl imidazolium

bromide [C_{14}MIM][Br] ionic liquid on the surface of Fe_3O_4 and their applicability for removal of reactive orange 122 as an anionic dye from aqueous samples was investigated. After magnetic separation, the target species can be easily removed from NPs by desorbing agents, and the recovered MNPs can be reused.

EXPERIMENTAL SECTION

Chemicals and reagents

All chemicals were of analytical reagent grade. Sodium hydroxide, hydrochloric acid, methanol, ethanol, propanol, $\text{FeCl}_3 \cdot 6\text{H}_2\text{O}$, $\text{FeCl}_2 \cdot 4\text{H}_2\text{O}$ with the highest purity purchased from Merck (Merck, Darmstadt, Germany). Reactive orange 122 (Fig. 1) was purchased with industrial purity. The ionic liquid [C_{14}MIM][Br] was synthesized in Chemistry and Chemical Engineering Research Center of Iran with high purity (>99.8%). Stock solution of dye with the concentration of 1000 mg/L was prepared by dissolving the powder in double distilled water. Working solutions were obtained daily by appropriately diluting the stock solutions with deionized water.

Apparatus

Absorbance measurements were obtained using an 8453 diode array UV Vis spectrophotometer (Agilent, USA). A 780 pH meter (Metrohm, Switzerland) was used for monitoring the pH values. The XRD measurements were performed on the XRD D8 Advance (Bruker, Germany). Scanning Electron Microscopy (SEM) was used to investigate the surface morphology of the synthesized adsorbent using the SEM model S4160 Cold Field Emission (Hitachi, Japan). Specific surface area and porosity were defined by N_2 adsorption-desorption porosimetry (77 K) using a Belsorp mini II BET surface area analyzer (Bel, Japan). A mechanical stirrer (Heidolph, Germany) was applied for stirring of the dye solutions with a glassware stirrer. The FTIR spectra were recorded on a FTIR spectrometer model spectrum 65 (Perkin-Elmer, UK). Thermogravimetric analyses were performed using a TG209F1A thermogravimetric analyzer (Netzsch, Germany). A super magnet Nd-Fe-B (1.4 T, 10 cm × 5 cm × 2 cm) for settlement of MNPs was also used.

Synthesis of Fe_3O_4 NPs

Fe_3O_4 NPs were prepared by mixing $\text{FeCl}_2 \cdot 4\text{H}_2\text{O}$ (2.74 g), $\text{FeCl}_3 \cdot 6\text{H}_2\text{O}$ (3.11 g) and 0.85 mL concentrated

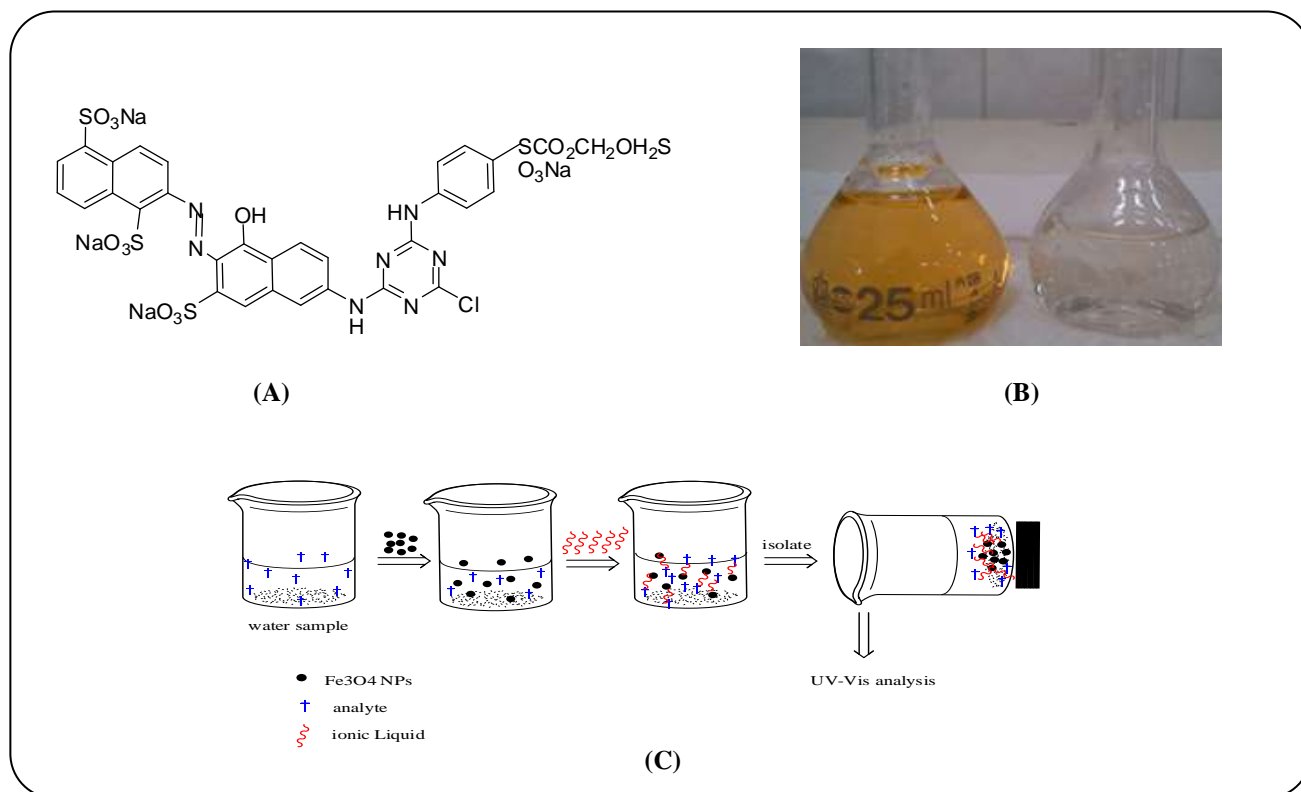


Fig. 1: (A) chemical structure of reactive orange 122, (B) dye solution with the concentration of 20 mg/L after and before removal, and (C) removal procedure of RO-122 by IL-Fe₃O₄.

hydrochloric acid into 25 mL deionized water. The mixture was added to a stirred 250 mL NaOH solution (1.5 M). In the designed method, the synthesis of MNPs was done by introducing nitrogen gas through a sparger into the solution for oxygen removal. The bubbling of nitrogen gas through the solution protects Fe₃O₄ against critical oxidation and reduces the particles size when compared to synthesis methods without oxygen removal [20]. During the whole process, the solution temperature was maintained at 80°C. After completion of the reaction, the obtained Fe₃O₄ NPs were separated from the reaction medium by the magnetic field, and then washed with 500 mL deionized water four times. The pH of suspension after the washings was 10 and concentration of the generated MNPs in suspension was estimated to be about 10 mg mL⁻¹ by weighing dried MNPs. The obtained MNPs were stable in this condition up to one month.

Dye removal experiments

In the proposed procedure, to achieve maximum adsorption efficiency, various parameters affecting

the removal of dye were studied and optimized with a univariate method. Each test consisted of preparing a 25 mL of dye solution with a desired initial concentration by diluting the stock dye solutions with deionized water. A known amount of IL-Fe₃O₄ was then added to the solution, and the obtained suspension was immediately stirred vigorously for a predefined time by a glassy rod. The dye loaded IL-Fe₃O₄ was then separated magnetically. The dye solution became colorless after stripping. The mixture was decanted and the supernatant was removed completely (Fig. 1). Removal percent and adsorbed amount of dye was determined spectrophotometrically by measuring the absorbance of the sample solutions before and after removing process at appropriate wavelengths corresponding to the maximum absorbance which is 288 nm for RO-122 dye. The following equation was applied to calculate the dye removal efficiency:

$$\%R = \frac{(C_0 - C_t)}{C_0} \times 100 \quad (1)$$

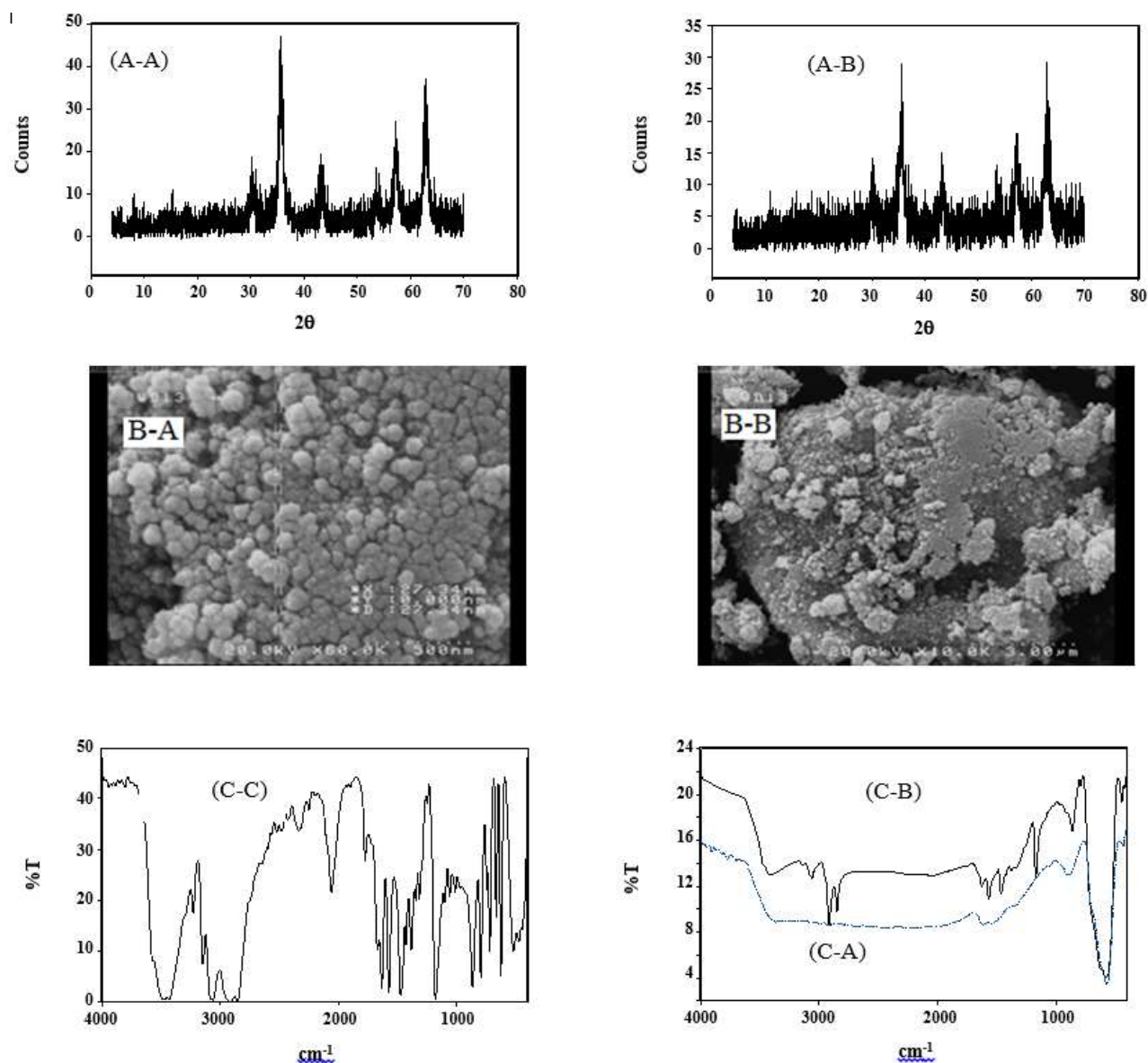


Fig. 2: (A-A) and (A-B) are XRD patterns of Fe_3O_4 and $IL-Fe_3O_4$, respectively. (B-A) and (B-B) are SEM images of Fe_3O_4 . (C-A), (C-B), and (C-C) are FT-IR spectra of the Fe_3O_4 , $IL-Fe_3O_4$, and $[C_{14}MIM][Br]$, respectively.

Where C_0 and C_t are the initial and residual concentrations of dye in the solution (mg/L), respectively.

RESULTS AND DISCUSSIONS

Characterization of Fe_3O_4 and $IL-Fe_3O_4$

The typical XRD profile of both $IL-Fe_3O_4$ and standard Fe_3O_4 are shown in Fig. 2 for comparison. Although the magnetic nanoparticle surfaces in $IL-Fe_3O_4$

were coated with ionic liquid, analysis of XRD patterns of both Fe_3O_4 and $IL-Fe_3O_4$ indicated very distinguishable peaks for magnetite crystal, which means that these particles have phase stability. We calculated the crystallite size measurement around 16.8nm from the XRD pattern according to Scherrer equation:

$$D = \frac{K\lambda}{b\cos\theta} \quad (2)$$

The equation uses the reference peak width at angle θ , where λ is the wavelength of incident X-ray (1.5418Å), b is the width of the XRD peak at half height and K is a shape factor, which is about 0.9 for magnetite and maghemite. The absence of the Fe_2O_3 peaks ranging from a 2θ angle of 20° to 30° proved that the black powder was Fe_3O_4 and therefore we can see that no impurities of Fe_2O_3 were observed.

The morphology of Fe_3O_4 was observed by SEM. As shown in Fig. 2, the well-shaped particles with diameter about 27 nm were achieved. It should be noted that the particle dimension obtained by SEM is higher than the corresponding crystallite size, i.e. 16.8 nm. This difference may be explained due to the presence of aggregates in SEM grain consisting of several crystallites and/or poor crystallinity.

IR spectra of Fe_3O_4 , IL- Fe_3O_4 and $[\text{C}_{14}\text{MIM}][\text{Br}]$ ionic liquid are shown in Fig. 2. The band at 3455 cm^{-1} is attributed to the stretching vibrations of $-\text{OH}$, which is assigned to surface OH groups of Fe_3O_4 NPs and the bands at low wavenumbers ($\leq 700\text{ cm}^{-1}$) are related to vibrations of the Fe-O bonds in iron oxide. The absorption band of Fe-O bonds of the bulk magnetite is observed at 570.9 cm^{-1} . The IR spectra show that the surface of Fe_3O_4 NPs was well modified by ionic liquid.

To estimate the amount of ionic liquid deposited onto the surface of Fe_3O_4 , the ThermoGravimetric Analysis (TGA) of Fe_3O_4 and IL- Fe_3O_4 was conducted. Fig. 3 shows the TGA curves of both Fe_3O_4 and IL- Fe_3O_4 nanoparticles. The first mass losses steps, to 140°C , are due to the loss of physically adsorbed water on the surfaces. The second mass losses steps, from 200 to about 800°C , are due to the decomposition of immobilized ionic liquid. According to the TGA curves, the ionic liquid content of IL- Fe_3O_4 nanoparticles was evaluated to be 27.9% by weight.

Specific surface area was determined by applying the theory of Brunauer, Emmett, and Teller (BET) to nitrogen adsorption/desorption isotherms measured at 77 K. The specific surface area of the sample is determined by physical adsorption of a gas on the surface of the solid and by measuring the amount of adsorbed gas corresponding to a monomolecular layer on the surface. The data are treated according to the BET theory. The results of the BET method in Fig. 4 showed that the average specific surface area of MNPs was $89.95\text{ m}^2/\text{g}$.

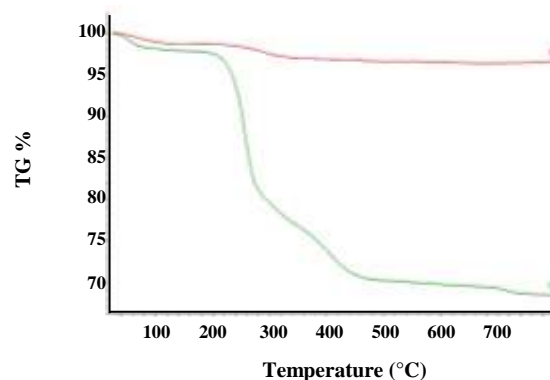


Fig. 3: TGA curves of the Fe_3O_4 , (A); and IL- Fe_3O_4 , (B). Temperature range: $20\text{--}800^\circ\text{C}$ (ramp $15^\circ\text{C}/\text{min}$), O_2

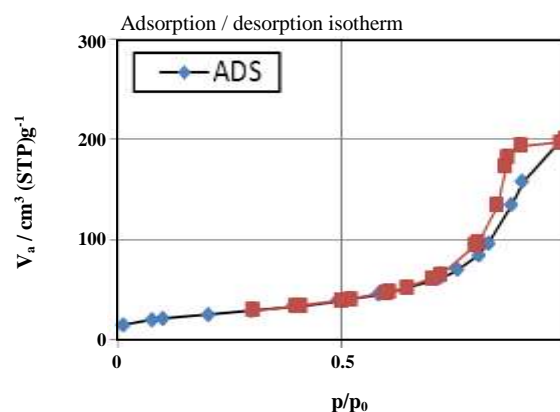


Fig. 4: Adsorption/desorption isotherm.

It can be concluded from these values that the synthesized magnetite is nanoparticles with relatively large specific surface area and the mean pore diameter was 10.37nm, with a total pore volume of $0.2116\text{ cm}^3/\text{g}$.

Effect of solution pH

pH is one of the prime factors influencing the adsorption behavior of mixed hemimicelles system. The solution pH would affect both aqueous chemistry and surface binding sites of the adsorbent [3]. The effect of pH of the solution, on the adsorption of RO-122 onto IL- Fe_3O_4 surfaces was assessed at different pH values, ranging from 3.0 to 12.0. The surfaces of metal oxides are generally covered with hydroxyl groups that vary in form with pH. At pHs more than about 7, the surface of MNPs is negatively charged, which increases the positively charged ionic liquid coating through electrostatic forces as double layer aggregations so called admicelles.

Also, electrostatic attraction between the positively charged surfactant and the negatively charged dye increases. According to the Fig. 5A, pH 10 was selected for all further adsorption experiments.

Effect of ionic liquid and MNPs amount

The effect of IL-Fe₃O₄ dosage on removal of RO-122 was investigated using a batch mode by adding a known quantity of the adsorbent, in the range of 0.2-2.0 mL. The results (Figure 5B) showed that the adsorption efficiencies increased by increasing adsorbent dose. This observation can be explained by the greater number of adsorption sites made available at greater MNPs dosages.

Fig. 5C depicts the percentage of adsorbed RO-122 as a function of the amount of [C₁₄MIM][Br] added. In the absence of [C₁₄MIM][Br], the RO-122 hardly adsorbed onto the surface of Fe₃O₄NPs. In contrast, with increase in [C₁₄MIM][Br], the sorption amount of RO-122 increased remarkably but at higher amounts of [C₁₄MIM][Br], the adsorption of RO-122 decreased gradually due to formation of ionic liquid (IL) aggregates in the solution which can compete with formation of IL aggregates on the surface of Fe₃O₄. Results of the present study indicated clearly that the hydrophobic interactions played an important role in the adsorption process. So, 0.6mL of [C₁₄MIM][Br] with the concentration of 1000 mg.L⁻¹ was chosen as optimum amount in order to achieve the highest possible extraction efficiency.

Effect of contact time

The contact time between adsorbate and adsorbent is one of the most important design parameters that affect the adsorption processes. The effect of contact time on the performance of IL-Fe₃O₄ in adsorbing RO-122 was investigated (Fig. 5D). The optimum contact time between sample solution and IL-Fe₃O₄ nanoparticles was considered to be 8 min. The fast adsorption rates could be referred to the absence of internal diffusion resistance [21]. The shorter the contact time in an adsorption system, the lower would be the capital and operational costs for real-world applications.

Ionic strength

Since the presence of any ion could affect the hydrophobic and electrostatic interaction between dyes and surface of IL-Fe₃O₄, the effect of solution ionic

strength on removal of RO-122 was investigated. Selected amount of NaCl in the range of 0.2–2.0%(w/v) was added to individual beakers containing 25 mL of the tested dye solution. According to the results, the presence of high ionic content reduces the dye removal efficiency. This phenomenon can be explained by the competition of anionic dye and Cl⁻ ion for the sorption sites. Thus, the strategy of no salt addition was performed for the kinetic and isotherm studies.

Desorption studies

The desorption study is very important since the regeneration of adsorbent decides the economic success of the adsorption process. Primary objective of regeneration is to restore the adsorption capacity of exhausted adsorbent while the secondary objective is to recover valuable components present in the adsorbed phase (e.g. dye). Organic solvents are known to disrupt surfactant aggregates [22]. Dye desorption from the IL-Fe₃O₄ was conducted by washing the dye loaded IL-Fe₃O₄ using 3.0 mL of methanol, ethanol and propanol, separately for the extraction from 30 mL of aqueous solution. In this study, 54% of RO-122 could be desorbed and recovered by propanol, 68% by ethanol and 90% by pure methanol, so methanol was chosen as the optimum desorption solvent. Addition of desorbing solution in multiple steps (3 steps) can improve the desorption process as expected. Therefore, enrichment factor of 10 and enhancement factor of 9 were achieved in solid phase extraction using methanol as eluent.

Adsorption isotherms

The isotherm models are important for describing the interactive behavior between solutes and adsorbent. The parameters obtained from different models provide important information on the sorption mechanisms and the surface properties and affinities of the sorbent. Since the more common models used to investigate the adsorption isotherm are Langmuir and Freundlich equations, the experimental results of this study were fitted with these two models.

The widely used Langmuir isotherm is based on the assumption that maximum adsorption corresponds to a saturated monolayer of adsorbate molecules on adsorbent surface with a constant energy [23]. The general form of the Langmuir isotherm is:

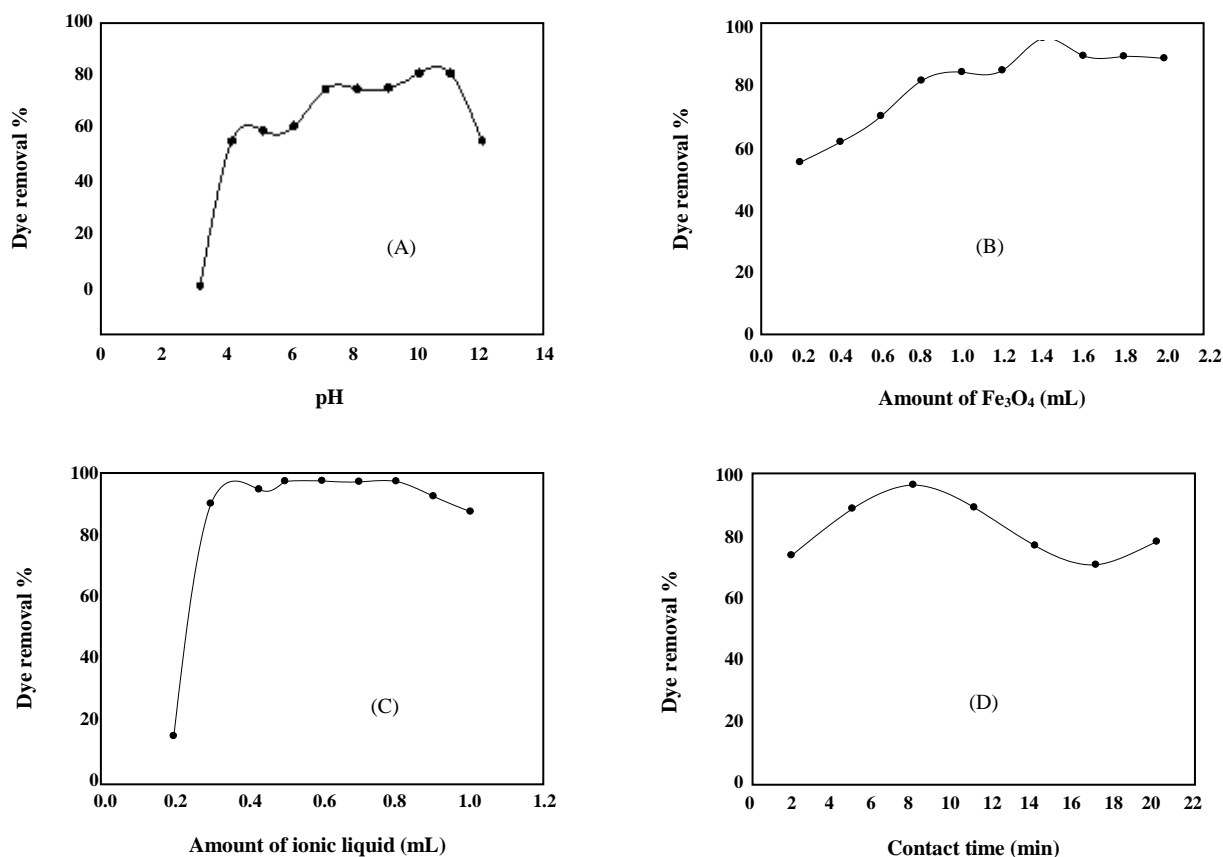


Fig. 5: Effect of (A) pH of dye solution, (B) dosage of IL-Fe₃O₄ nanoparticles, (C) ionic liquid amount, and (D) contact time on removal of RO-122. Experimental conditions: initial dyes concentrations of 20 mg/L and stirring time of 5 min. (primary conditions: 25 mL of 20mg/L dye solution, 0.6 mL of ionic liquid solution and 5 minutes as extraction time).

$$\frac{c_e}{q_e} = \left(\frac{1}{bq_{\max}} \right) + \left(\frac{C_e}{q_{\max}} \right) \quad (3)$$

Where q_e is the amount of dye adsorbed per unit mass of adsorbent (mg/g), C_e is the equilibrium concentration of dye in the solution (mg/L), b is the Langmuir constant (L/mg) and q_{\max} is the maximum adsorption capacity (mg/g).

The well-known Freundlich isotherm is often used for heterogeneous surface energy systems. It considers multilayer adsorption with a heterogeneous energetic distribution of active sites, accompanied by interactions between adsorbed molecules. The Freundlich empirical model is represented by:

$$\ln q_e = \ln k_f + \left(\frac{1}{n} \right) \ln C_e \quad (4)$$

Where q_e is the amount adsorbed at equilibrium (mg/g), C_e is the equilibrium concentration (mg/L), and K_f (mg^{1-1/n}L^{1/n}g⁻¹) and $1/n$ are Freundlich constants.

The amount of adsorption at equilibrium, q_e (mg/g), was calculated by:

$$q_e = \frac{V(C_0 - C_e)}{m} \quad (5)$$

Where C_0 and C_e are the initial and equilibrium concentrations of dye in (mg/L) respectively, V is the volume of experimental solution in L, and m is the dry weight of nanoparticles in g.

The favorability of the dye adsorption process onto MNPs was evaluated using a dimensionless parameter (R_L) derived from the Langmuir expression. It is defined as follows:

$$R = \frac{1}{(1 + bC_0)} \quad (6)$$

Table 1: Adsorption isotherms parameters of RO-122 onto IL-Fe₃O₄

Langmuir model					Freundlich model		
q _{max} (mg/g)	b	k _L (L/mg)	R	Correlation coefficient	k _f (L/mg)	N	Correlation coefficient
51.546	2.55	131.57	0.02	0.890	34.956	1.55	0.944

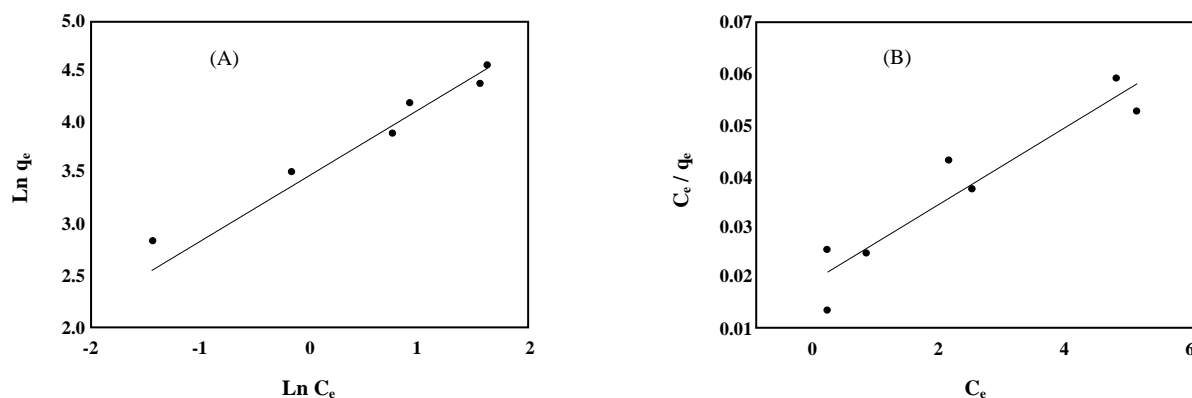


Fig. 6: Equilibrium isotherms plots; (A) Freundlich isotherm plot; (B) Langmuir isotherm plot. Concentration range: 5-60mgL⁻¹ and pH=10, 25 mL sample volume.

Which b parameter is a coefficient related to the energy of adsorption and increases by increasing strength of the adsorption bond. The adsorption process can be defined as irreversible ($R_L=0$), favorable ($0 < R_L < 1$), linear ($R_L=1$) or unfavorable ($R_L > 1$) in terms of R_L .

The calculated parameters for Langmuir and Freundlich isotherms and the correlation coefficients (r) are listed in Table 1. Results according to Fig. 6 show that the values of correlation coefficient, r , for fitting of experimental isotherm data to Freundlich equation is more close to 1.0000 than that for Langmuir equation. Therefore, the Freundlich model represents the experimental data better on the basis of values of regression coefficients. This model describes the multilayer adsorption of the solute on heterogeneous surface of the adsorbent.

Kinetic studies

The study of kinetics of dye adsorption onto Fe₃O₄NPs is required for selecting optimum operating conditions for the full-scale bath processes. Kinetic studies were performed in a 0.5 L glass beaker where 11.2mL of 10 mg/mL of Fe₃O₄ suspension and 4.8 mL of 1g/L of [C₁₄MIM][Br] solution were added into 200 mL of dye solution with the concentration of 50 (mg/L)

at ambient temperature. At preset time intervals, ranged from 2 to 60 min, the samples of 5 mL were taken from the solution and then the clear supernatant solutions were analyzed for residual RO-122 concentration in the solution. Fig. 7 shows the influence of time on the dye removal. The removal rate was very fast during the initial stages of the adsorption processes. The time required to achieve the adsorption equilibrium was only 38 minutes. To describe the adsorption behavior and rate, the data obtained from adsorption kinetic experiments were evaluated using pseudo-first- and pseudo-second-order reaction rate models.

The rate of pseudo-second order reaction may be dependent on the amount of solute adsorbed on the surface of adsorbent and the amount adsorbed at equilibrium [24]. The kinetic rate equations for pseudo-second order reaction can be written as follows:

$$\frac{t}{q_t} = \frac{1}{K_2 q_e^2} + \left(\frac{1}{q_e}\right)t \quad (7)$$

Where q_t and q_e , are the value of adsorbed dye (mg/g) at each time and at equilibrium, respectively, and K_2 is the equilibrium rate constant of pseudo-second-order adsorption (g/mg min).

Table 2: Adsorption kinetic parameters of RO-122 onto IL-Fe3O4

Pseudo second order	Initial concentration	Equation	$q_e(\text{mg/g}^{-1})$	$K(\text{g/mg min})$	Correlation coefficient
	47mg/L ⁻¹	$t/q_t=0.0127t+0.0304$	78.7	0.0053	0.9975
Pseudo first order	Initial concentration	Equation	$q_e(\text{mg.g}^{-1})$	$K(\text{min}^{-1})$	Correlation coefficient
	47mg L ⁻¹	$3.84+0.1071=-\ln(q_e-q_t)$	46.62	0.1071	0.8640

Table 3: Figures of merit of the proposed method.

(RSD%)	LOQ ($\mu\text{g/L}$)	LOD ($\mu\text{g/L}$)	Correlation coefficient	Dynamic linear range (mg/L)	Calibration equation
2.9%	46	14	0.9995	0.05-50	$Y=0.0245X+0.0061$

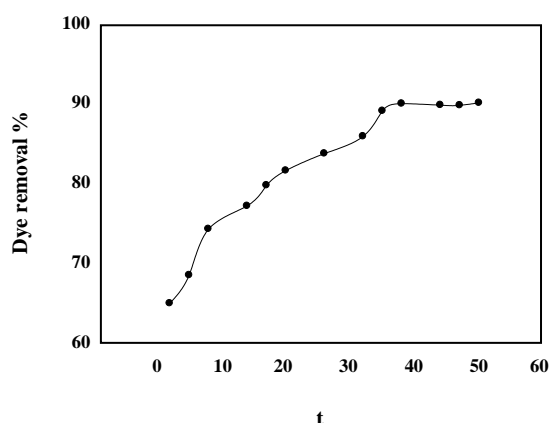


Fig. 7: Effect of time on the removal efficiency.

The pseudo-first-order model can describe different adsorption situations, such as systems close to equilibrium; systems with time-independent solute concentration or linear equilibrium adsorption isotherm; and more complex systems [22]. This model is represented by:

$$\ln(q_e - q_t) = \ln q_e - K_1 t \quad (8)$$

Where K_1 is the equilibrium rate constant of pseudo-first-order sorption (1/min). The slope and intercept of the plot of $\ln(q_e - q_t)$ versus t are used to determine the first-order rate constant, K_1 . The kinetic results are shown in Table 2 and Fig. 8.

Analytical features

The analytical features of the proposed method such as precision, linearity range of calibration curve and limit of detection were also examined. The results are summarized in Table 3. The removal of RO-122 was quantitative (>98%) and the precision of the method

was very good (RSD = 2.9%). The linear calibration range for measurements under the optimum conditions was 0.05–50 mg/L ($R^2 = 0.9995$). The detection limit based on six times of the standard deviation of the blank solution (3Sb/m) was found to be 14 $\mu\text{g/L}$.

Analysis of environmental water samples

In order to check the applicability of the proposed method for various water samples, RO-122 was determined in different water samples including Tehran tap water, well water (Chitgar, Tehran) and river water (Vardavard, Tehran). An appropriate volume of sample solution was adjusted to the optimum pH and subjected to the recommended procedure. Reliability was checked by spiking samples. Water samples spiked with 10, 15 and 20 mg/L of RO-122, were extracted by the proposed procedure. Table 4 lists the recoveries and concentrations found for RO-122, expressed as the mean value ($n = 3$). Recoveries ranged between 87.5% and 95.1% for the all four water samples. The results demonstrate the applicability of the proposed method to water analysis.

CONCLUSIONS

The sorption of pollutants from aqueous solutions plays a significant role in water pollution control. For this purpose, novel magnetic nano-adsorbent was fabricated by modifying the surface of $\text{Fe}_3\text{O}_4\text{NPs}$ with $[\text{C}_{14}\text{MIM}][\text{Br}]$ ionic liquid. The prepared magnetic adsorbent can be well dispersed in the water and can be easily separated magnetically from the medium after adsorption. Unique features such as high adsorption capacity, stability, reusability and ease of synthesis present this adsorbent as a promising and feasible alternative for dye removal. In addition, it should not be forgotten that the IL- Fe_3O_4 NPs adsorbent was

magnetically recoverable. This function will be quite useful in practical applications and will reduce time-consumption.

Received : Oct. 22, 2014 ; Accepted : Sep. 28, 2015

REFERENCES

- [1] Parham H., Zargar B., Heidari Z., Hatamie A., [Magnetic Solid-Phase Extraction of Rose Bengal Using Iron Oxide Nanoparticles Modified with Cetyltrimethylammonium Bromide](#), *Journal of the Iranian Chemical Society*, **8**: 9-16 (2011).
- [2] Zhang W., Yang H., Dong L., Yan H., Li H., Jiang Z., Kan X., Li A., Cheng R., [Efficient Removal of Both Cationic and Anionic Dyes from Aqueous Solutions Using A Novel Amphoteric Straw-Based Adsorbent](#), *Carbohydrate Polymers*, **90**: 887-893 (2012).
- [3] Afkhami A., Saber-Tehrani M., Bagheri H., [Modified Maghemite Nanoparticles as an Efficient Adsorbent for Removing Some Cationic Dyes from Aqueous Solution](#), *Desalination*, **263**: 240-248 (2010).
- [4] Golder A., Hridaya N., Samanta A., Ray S., [Electrocoagulation of Methylene Blue and Eosin Yellowish Using Mild Steel Electrodes](#), *Journal of Hazardous Material*, **127**: 134- (2005).
- [5] Daraei, A., [Treatment of Textile Wastewater with Organoclay](#), *Iranian Journal of Chemistry and Chemical Engineering (IJCCE)*, **32**: 67-70 (2013).
- [6] Afkhami A., Madrakian T., Amini A., Karimi Z., [Effect of the Impregnation of Carbon Cloth with Ethylenediaminetetraacetic Acid on Its Adsorption Capacity for the Adsorption of Several Metal Ions](#), *Journal of Hazardous Material*, **150**: 408-412 (2008).
- [7] Samarghandi MR., Zarrabi M., Noori Sepehr M., Panahi R., Foroghi M., [Removal of Acid Red 14 by Pumice Stone as a Low Cost Adsorbent: Kinetic and Equilibrium Study](#), *Iranian Journal of Chemistry and Chemical Engineering (IJCCE)*, **31**: 19-27 (2012).
- [8] Ishaq M., Saeed K., Ahmad I., Sultan S., Akhtar S., [Coal Ash as a Low Cost Adsorbent for the Removal of Xylenol Orange from Aqueous Solution](#), *Iranian Journal of Chemistry and Chemical Engineering (IJCCE)*, **33**: 53-58 (2014).
- [9] Chang YC., Chen DH., [Adsorption Kinetics and Thermodynamics of Acid Dyes on A Carboxymethylated Chitosan-Conjugated Magnetic Nano-Adsorbent](#), *Macromolecular Bioscience*, **5**: 254-261 (2005).
- [10] Faraji M., Yamini Y., Rezaee M., [Magnetic Nanoparticles: Synthesis, Stabilization, Functionalization, Characterization, and Applications](#), *Journal of the Iranian Chemical Society*, **7**: 1-37 (2010).
- [11] Lu AH., Salabas EeL., Schüth F., [Magnetic Nanoparticles: Synthesis, Protection, Functionalization, and Application](#), *Angewandte Chemie International Edition*, **46**: 1222-1244 (2007).
- [12] Kaur S., Gaur A., [Structural and Photoluminescence Study of Iron Oxide Nanoparticles](#), *Advanced Science Letters*, **20**: 1707-1709(2014).
- [13] Takafuji M., Ide S., Ihara H., Xu Z., [Preparation of Poly \(1-vinylimidazole\)-grafted Magnetic Nanoparticles and their Application for Removal of Metal Ions](#), *Chemistry of Materials*, **16**: 1977-1983 (2004).
- [14] Racles C., Iacob M., Butnaru M., Sacarescu L., Cazacu, M., [Aqueous Dispersion of Metal Oxide Nanoparticles, Using Siloxane Surfactants](#), *Colloids and Surfaces A: Physicochemical and Engineering Aspects* **448**: 160-168 (2014).
- [15] Zhang C., Shan C., Jin, Y., Tong, M., [Enhanced Removal of Trace Arsenate by Magnetic Nanoparticles Modified with Arginine and lysine](#), *Chemical Engineering Journal* **254**: 340-348 (2014).
- [16] Zhang Q., Yang F., Tang F., Zeng K., Wu K., Cai Q., Yao S., [Ionic Liquid-Coated Fe₃O₄ Magnetic Nanoparticles as an Adsorbent of Mixed Hemimicelles Solid-Phase Extraction for Preconcentration of Polycyclic Aromatic Hydrocarbons in Environmental Samples](#), *Analyst*, **135**: 2426-2433 (2010).
- [17] Galán-Cano F., del Carmen Alcudia-León M., Lucena R., Cárdenas S., Valcárcel M., [Ionic Liquid Coated Magnetic Nanoparticles for the Gas Chromatography/Mass Spectrometric Determination of Polycyclic Aromatic Hydrocarbons in Waters](#), *Journal of Chromatography A*, **1300**: 134-140 (2013).
- [18] Vidal L., Riekkola M. L., Canals A., [Ionic Liquid-Modified Materials for Solid-Phase Extraction and Separation: A review](#), *Analytica Chimica Acta*, **715**: 19-41 (2012).

- [19] Berthod A., Ruiz-Angel M., Carda-Broch S., [Ionic Liquids in Separation Techniques](#), *Journal of Chromatography A*, **1184**: 6-18 (2008).
- [20] Mandel, K., Hutter F., Gellermann C., Sendl G., [Synthesis and Stabilisation of Superparamagnetic Iron Oxide Nanoparticle Dispersions](#), *Colloids and Surfaces A: Physicochemical and Engineering Aspects*, **390**: 173-178 (2011).
- [21] Zargar B., Parham H., Hatamie A., [Fast Removal and Recovery of Amaranth by Modified Iron Oxide Magnetic Nanoparticles](#), *Chemosphere*, **76**, 554-557 (2009).
- [22] Shariati S., Faraji M., Yamini Y., Rajabi AA., [Fe₃O₄ Magnetic Nanoparticles Modified with Sodium Dodecyl Sulfate for Removal of Safranin O Dye from Aqueous Solutions](#), *Desalination*, **270**: 160-165 (2011).
- [23] Afkhani A., Moosavi R., [Adsorptive Removal of Congo Red, a Carcinogenic Textile Dye, from Aqueous Solutions by Maghemite Nanoparticles](#), *Journal of Hazardous Material*, **174**: 398-403 (2010).
- [24] Faghihian H., Rasekh M., [Removal of Chromate from Aqueous Solution by a Novel Clinoptilolite-Polyaniline Composite](#), *Iranian Journal of Chemistry and Chemical Engineering (IJCCE)*, **33**(1): 45-51 (2014).